Journal of Material Cycles and Waste Management (2022) 24:1267–1280
https://doi.org/10.1007/s10163-022-01399-5

SPECIAL FEATURE: ORIGINAL ARTICLE

Material Cycles in Construction Works

# Utilization of high-volume mine tailing and by-products in composite binder production: hardened properties and sustainable development

Duy-Hai Vo[1,3] · Chao-Lung Hwang[2] · Khanh-Dung Tran Thi[3] · Mitiku Damtie Yehualaw[4] · Min-Chih Liao[3] · Yun-Tai Lee[3]

Received: 14 August 2021 / Accepted: 1 March 2022 / Published online: 16 April 2022


## Abstract

This study was designed to investigate the hardened performance of the paste specimens produced using a composite binder with high volumes of mine tailings incorporating various by-products. Mine tailing and fly ash (FA) content was tested at 40%, 50%, and 60% of total paste volume, and tailing pastes were produced at w/b ratios of 0.12, 0.16, and 0.2. To reduce the usage of cement, Portland cement was replaced by ground granulated blast furnace slag (GGBFS) at 10%, 30% and 50% of cement weight and, to modify the paste properties, silica fume (SF) was added at 5%, 10%, and 15% of the binder mass. The hardened performance of the tailing paste specimens was evaluated in terms of compressive strength, thermal conductivity (TC), ultrasonic pulse velocity (UPV), water absorption (WA), sulfate attack resistance, and SEM analysis was used to examine the microstructure. After 56 days of curing, the tailing paste obtained high compressive strength results ranging between 34.2 and 86.2 MPa. The paste samples with lower tailing and GGBFS content and lower w/b ratios exhibited better hardened properties and denser morphologies. Finally, adding 5% SF was found to significantly improve the microstructure and mechanical properties of the paste specimens.

**Keywords** Mine tailing paste · Compressive strength · Sulfate resistance · By-products

## Introduction

Ordinary Portland cement (OPC) is the main binder used in concrete production worldwide. Demand for cement is expected to continue rising through the coming decades, with demand for cement in 2020 reaching 115–180% and demand in 2050 expected to reach 400% of levels in the 1990s [1]. Cement production presents many challenges in terms of energy and natural resources consumption as well as emissions of $CO_2$ [2]. The cement manufacturing process consumes around 1.7 tonnes of raw materials and releases 1 tonne of $CO_2$ for every 1 tonne of clinker produced. Moreover, this process generates some 5–8% of man-made $CO_2$ emissions [3, 4]. The major role played by $CO_2$ emissions in global warming is encouraging researchers to assess potential greener alternatives to cement to reduce cement consumption. Besides, concrete structures in an underground environment are usually exposed to various chemical substances, including sulfate and chloride, which are ubiquitous in soil, groundwater and seawater and are damaging [5]. It has long been recognized that sulfate attack usually results in the formation of expansive products, such as ettringite, gypsum, and thaumasite, which are produced by sulfate ions reacting with hydration products in cement, resulting in expansion, cracking, spalling, and concrete strength loss and affect to the durability of concrete samples [6–8]. Using supplementary cementitious materials (SCM) such as silica fume, GGBFS, and fly ash as pozzolanic materials for partial replacement in cement has been reported in many studies to

✉ Min-Chih Liao
minchih.liao@mail.ntust.edu.tw

1 Faculty of Civil Engineering, University of Technology and Education, The University of Danang, 48 Cao Thang Street, Hai Chau District, Danang City, Viet Nam

2 Taiwan Building Technology Center, National Taiwan University of Science and Technology, No. 43, Sec. 4, Keelung Rd, Taipei 10607, Taiwan, ROC

3 Department of Civil and Construction Engineering, National Taiwan University of Science and Technology, No. 43, Sec. 4, Keelung Rd, Taipei 10607, Taiwan, ROC

4 Faculty of Civil and Water Resource Engineering, Bahir Dar Institute of Technology, Bahir Dar University, Bahir Dar, Ethiopia

produce cement with acceptable mechanical properties and durability and sulfate resistance [9–13]. However, the less-than-ideal physical properties and chemical compositions of SCM (e.g., low reactivity index, crystalline phase, and angular shape) frequently lead to concrete that has been produced with SCM as a partial replacement to exhibit problems such as low early-age compressive strength, significant autogenous shrinkage, and drying shrinkage [9, 10, 14]. Using ternary and quaternary binders with high-volume blends of industrial by-products such as GGBFS and FA is an area of potential eco-friendly cement development [15–18].

Vast amounts of mineral products are mined annually worldwide. In addition to minerals, mining generates large volumes of solid wastes such as waste rock, tailings, and slag [19]. Ore tailings are a byproduct of flotation, gravity concentration, and other mineral-separation processes [20–24]. The high heavy metal content in ore tailings regularly contributes to water resource contamination through leaching, and large amounts of land must be dedicated to the long-term storage of this material, posing threats to human safety and welfare [25–27]. Therefore, developing beneficial and safe uses for ore tailings is necessary to mitigate the negative impacts of this material.

Steadily increasing demand for copper, an important metal in many fields of industrial manufacture, is driving growth in copper mining around the world. Copper mine tailings, a main byproduct of copper ore flotation processing [28], is causing extensive environmental pollution in many copper-mining countries. Around 30 million tonnes of copper mine tailings are discharged during engineering process of copper containing mine, worldwide [29]. As the chemical composition of copper mine tailings is similar to cementitious raw materials [30, 31], these tailings may be a viable alternative input material for the production of cement clinker. The potential for using copper mine tailing as a partial replacement for conventional cement has been examined in several previous studies [32, 33]. Onuaguluchi and Eren [34] investigated the effect of copper tailings as a partial cement replacement at levels from 0 to 15%. Their findings indicated that absorbed water and permeable voids increased and compressive strength and mechanical properties decreased at higher levels of copper tailing replacement. Moreover, at higher replacement levels, chemical resistance declined and thermal conductivity increased. Dandautiya and Singh [35] used blended fly ash and copper tailings as a partial replacement for cement, finding that although both FA and copper tailings met the requirements to be classified as pozzolanic materials, the cement samples exhibited steadily lower compressive strength values as the replacement level of blended tailings and FA content increased. The replacement level of 10% FA and 5% copper tailings showed higher compressive strength than the control mixture, and the replacement level of 20% FA and 5% copper tailings achieved a high compressive strength. Reusing FA and copper tailings in concrete production offers benefits in terms of lower production costs and reduced $CO_2$ emissions. S. Liu et al. [32] assessed the hydration properties of the composite binder of Portland cement by modifying the copper tailing powder using different grinding times. The hydration products included C–S–H gel, $Ca(OH)_2$, ettringite, $CaCO_3$, and dolomite. According to the test results, the $Ca(OH)_2$ content also declined as copper tailing powder levels increased. In addition, the superfluous $SiO_2$ in the copper tailing powder contributed to C–S–H gel formation via the reaction with $Ca^{2+}$, resulting in a larger volume of C–S–H gel at later ages. The proportion of copper tailings in the cement was shown to affect the mechanical properties and pore structure of the paste specimens. However, the focus of articles in the literature has mainly been on the hydration process of cement paste with relatively minor copper tailings modification ($\leq 30\%$). The hardened performance of composite binder that has been produced with copper tailings blended with other by-products is an issue that has received minimal research attention to date and thus deserves further study.

Using mine tailings as partial replacement in cement is attractive both for reducing the use of newly mined raw materials and for reusing a difficult-to-manage solid waste. However, utilization of high mine tailing volume in production of ternary or quaternary composite binder is not widely mentioned previous study. In addition, copper mine tailings contain high proportions of silica, alumina, and iron oxide (around 90% of the material by weight), which is higher than the requirement for Class N raw and calcined natural pozzolanas materials published in ASTM C618-15. Thus, copper mine tailings may be used in construction as a pozzolanic material. Therefore, this study was designed to provide detailed insights into the potential for using copper mine tailings in construction materials. Composite binder samples were produced by incorporating high volumes of copper mine tailings with other by-products such as FA, GGBFS, and silica fume, and various tests of the hardened properties of the tailing pastes were conducted up to 56 days of curing age.

## Materials and experimental methods

### Materials and mix proportions

In this study, ordinary Portland cement type I was used following ASTM C150. The tailing powder was collected from copper mine tailing slurry in China to use as a cementitious material. Three types of supplementary cementitious materials, including GGBFS, fly ash, and silica fume, were used to modify the tailing paste specimens, with details regarding the physical properties and chemical

**Table 1** Physical and chemical analyses of raw materials

| Materials | OPC | Tailing | FA | GGBFS | SF |
|---|---|---|---|---|---|
| *Chemical compositions* (%) | | | | | |
| $SiO_2$ | 21.82 | 76.33 | 63.22 | 36.7 | 97.54 |
| $Al_2O_3$ | 4.82 | 10.91 | 22.8 | 14.67 | 0.13 |
| $Fe_2O_3$ | 3.07 | 2.49 | 5.5 | 0.3 | 0.13 |
| CaO | 62.08 | 0.66 | 3.36 | 38.73 | 0.19 |
| MgO | 3.58 | 0.22 | 0.99 | 6.21 | 0.17 |
| $SO_3$ | 2.84 | 2.48 | 0.54 | 1.67 | 1.3 |
| $K_2O$ | 0.62 | 5.9 | 1.02 | 0.32 | 0.26 |
| $Na_2O$ | 0.41 | 0.44 | 1.13 | 0.34 | 0.24 |
| $P_2O_5$ | – | – | 0.29 | – | – |
| $TiO_2$ | 0.53 | 0.22 | 0.96 | 0.66 | – |
| MnO | 0.05 | – | – | 0.34 | – |
| Physical properties | | | | | |
| Specific gravity | 3.15 | 2.73 | 2.17 | 2.85 | 2.27 |
| D50 (μm) | 16.82 | 22.36 | 16.61 | 8.83 | 16.53 |

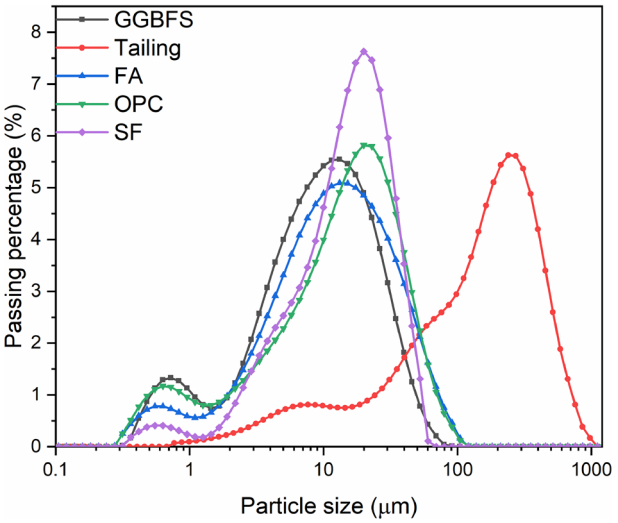


**Fig. 1** Cumulative distributions of raw materials

**Fig. 2** Mine tailing image

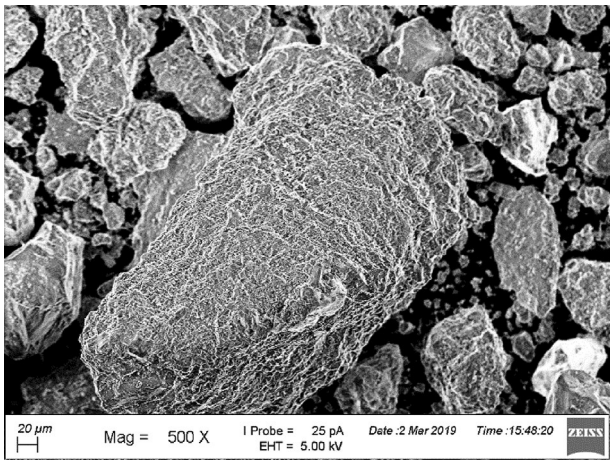


**Fig. 3** SEM image of mine tailing particles

compositions of these specimens displayed in Table 1. The particle size distributions of the raw materials are given in Fig. 1 and the tailing powder particles is shown in Fig. 2. The chemical compositions of these materials were analyzed using an X-ray fluorescence (XRF) spectrometer. As shown in Table 1, the mine tailing contained $SiO_2$, $Al_2O_3$, and $Fe_2O_3$ of 76.33%, 10.91%, and 2.49%, respectively and the total proportion of these three compounds was 89.73%, which is significantly higher than the 70% required under ASTM C618-15 for raw and calcined natural pozzolanic materials. The SEM image and XRD pattern of the tailing powders are shown in Figs. 3 and 4, respectively. Superplasticizer type G was used to achieve the desired level of workability in the paste samples, and the mixing water used was local tap water.

First, a composite binder was prepared by a mixture of mine tailing and fly ash with a ratio of 10% FA by the total weight of FA and mine tailing. This proportion was blended following Fuller's curve method, which determined the highest density of binder material based on the particle size distribution of FA and tailing. Then, the paste mixtures were produced with the high volume of mine tailing and FA (CT) with 40%, 50% and 60% compared with cement content. These mixtures were designed with a w/b ratio of 0.12. Next, the 50% CT mixture (xT0.5S00F0) was modified using w/b ratios of 0.16 and 0.2. To reduce the cement consumption, GGBFS was used to replace OPC in the mixture 0.12T0.5SxF0 at respective content ratios of 10%, 30%, and 50%. Finally, silica fume at 5%, 10%, and 15% of mixture

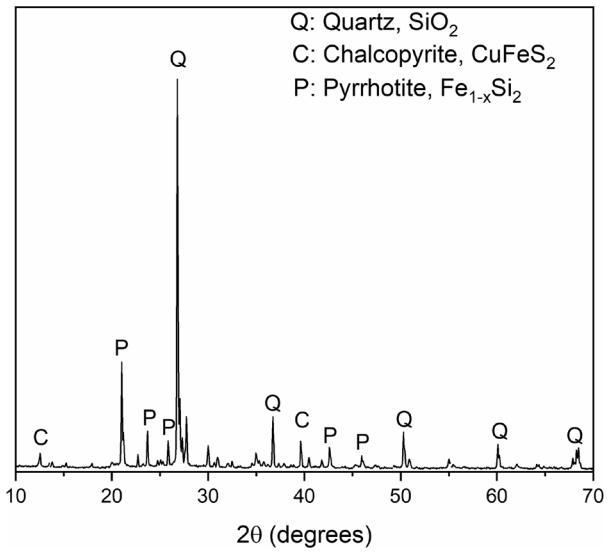


**Fig. 4** XRD analysis of mine tailing

weight was added to the mixture with 30% GGBFS content 0.12T0.5S30Fx to improve the performance of the tailing paste specimens. The detailed mixtures are presented in Table 2.

### Sample preparation and test program

After mixing, the tailing paste samples were made in two layers in 30 × 30 × 30 mm cubic molds and 50 × 100 mm cylinder molds, then shook for 3 min to remove voids with a vibration machine. A plastic thin film covered the surface of the molds after mixing to prevent evaporation. All the paste samples were demolded after 48 h and cured in a chamber maintained at a temperature of 25 ± 2 °C and a humidity level of 95% ± 5% until the testing day. The mechanical properties were tested for compressive strength in accordance with ASTM C109. The UPV test was conducted in accordance with ASTM C597 and the thermal conductivity analysis was done in controlled condition at a temperature of 25 ± 2 °C and a humidity level of 65% ± 5% within 10 min using an Isomet 2014 device with a surface probe fitted with a temperature sensor. Water absorption was measured by calculating the differences in mass of the paste specimens under oven-dried and saturated-surface-dry conditions. Sulfate attack resistance was measured by calculating the changes in mass of the specimens during a wetting and drying cycle in which the 28-day paste specimens were first immersed in a sulfate solution of 5% $Na_2SO_4$ for 1 day, and then heated in an oven at 105 ± 5 oC for 22 h, and then finally air cooled for 2 h. The mass change was observed for 10 consecutive wet–dry cycles. The resultant microstructure of the specimens was analyzed using SEM images taken with a scanning electron microscope (JEOL model JSM-6390LV). The X-ray diffraction was conducted using a BRUKER diffractometer model D2-PHASER that used CuKα radiation with step-scanned at 2θ in the ranges of 10–70°.

## Results and discussion

### Compressive strength

As shown in Fig. 5, compressive strength development in the tailing paste specimens increased with curing time (3 days to 56 days), with compressive strength values 34.5–120.2% higher at 56 days of curing than at 7 days of curing. This increase may be due to the pozzolanic reaction of the cement paste components at later curing days, which formed extra hydration product and improved the compressive strength results. As shown in Fig. 5 a, the paste samples containing 40% CT by volume exhibited the highest compressive strength at 56-day (86.2 MPa),

**Table 2** Mix proportions of tailing paste (kg/m$^3$)

| Mixtures | w/b | OPC | GGBFS | FA | SF | Tailing | Water | SP |
|---|---|---|---|---|---|---|---|---|
| 0.12T0.4S00F0 | 0.12 | 1080 | 0 | 107 | 0 | 958 | 257 | 21.4 |
| 0.12T0.5S00F0 | 0.12 | 778 | 0 | 133 | 0 | 1198 | 253 | 21.1 |
| 0.12T0.6S00F0 | 0.12 | 476 | 0 | 160 | 0 | 1437 | 249 | 20.7 |
| 0.12T0.5S10F0 | 0.12 | 700 | 78 | 133 | 0 | 1198 | 253 | 27.4 |
| 0.12T0.5S30F0 | 0.12 | 545 | 233 | 133 | 0 | 1198 | 253 | 27.4 |
| 0.12T0.5S50F0 | 0.12 | 389 | 389 | 133 | 0 | 1198 | 253 | 27.4 |
| 0.16T0.5S00F0 | 0.16 | 601 | 0 | 133 | 0 | 1198 | 309 | 19.3 |
| 0.20T0.5S00F0 | 0.2 | 452 | 0 | 133 | 0 | 1198 | 357 | 0 |
| 0.12T0.5S30F5 | 0.12 | 545 | 233 | 133 | 105 | 1198 | 253 | 33.2 |
| 0.12T0.5S30F10 | 0.12 | 545 | 233 | 133 | 211 | 1198 | 253 | 46.4 |
| 0.12T0.5S30F15 | 0.12 | 545 | 233 | 133 | 316 | 1198 | 253 | 60.6 |

Note: aTxSyFz with: a—w/b ratio, x—tailing and FA volume, y—GGBFS content, z—silica fume content

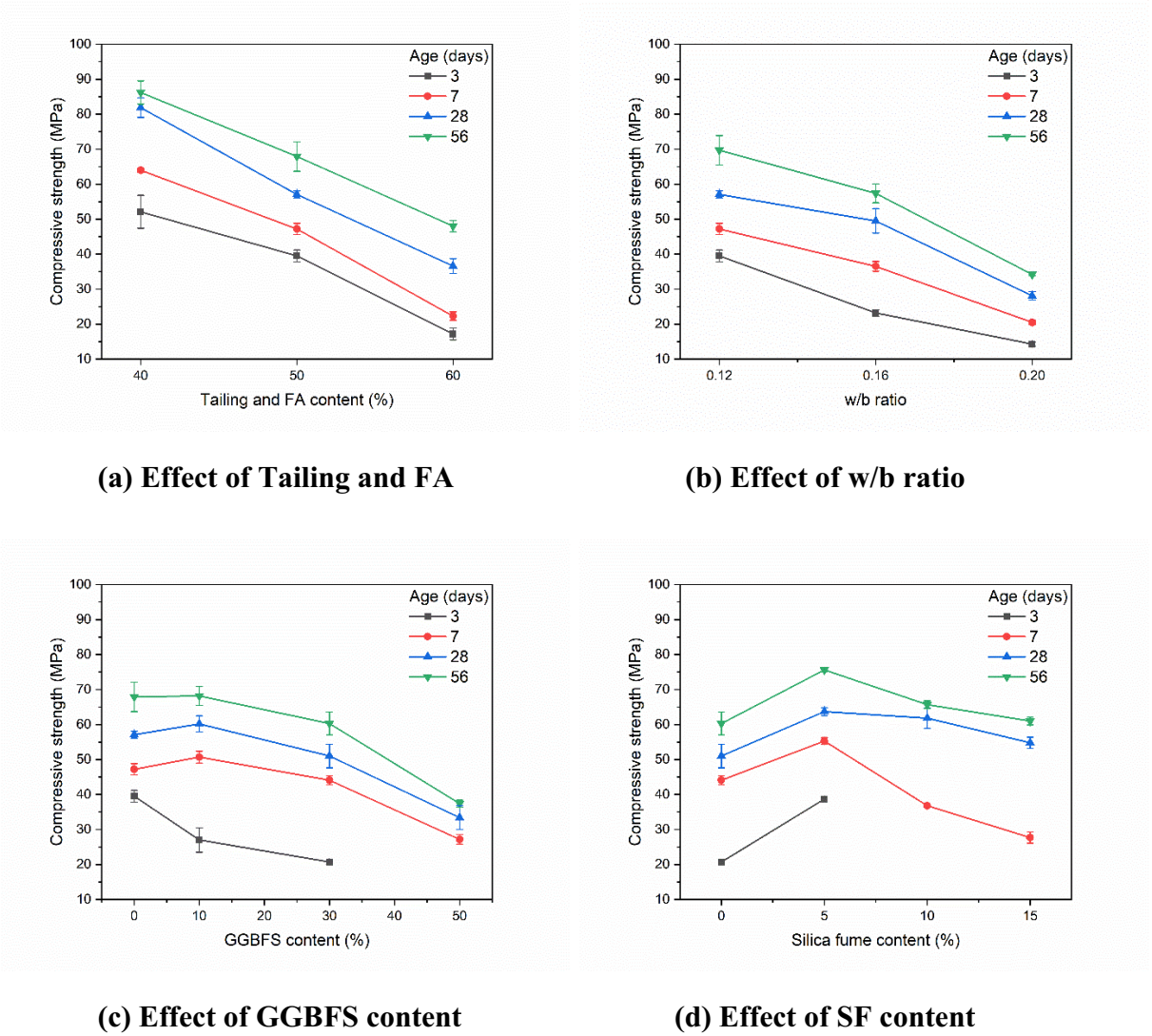


**Fig. 5** Compressive strength of tailing paste samples. **a** Effect of tailing and FA. **b** Effect of w/b ratio. **c** Effect of GGBFS content. **d** Effect of SF content

while the 50% and 60% CT mixtures exhibiting respective strengths of 67.9 MPa and 48 MPa. This result indicates that the compressive strength of tailing paste was significantly reduced with increased CT volume due to the low pozzolanic activity of the tailing and fly ash particles contributing less to the hydration process [36–38]. On the other hand, higher amounts of tailing particles increased the pore structure of the paste samples due to the negative effect of coarse tailing particles, which increased the critical pore diameter and reduced the mechanical properties of the cement paste specimens [39]. Besides, the larger CT volume reduced the content of cement (as shown in Table 2), leading to lower $Ca(OH)_2$ content levels, which affected hydration rate and strength development in the paste samples [40].

In addition, the w/b ratio was found to affect compressive strength significantly. As shown in Fig. 5b, increasing the w/b ratio from 0.12 to 0.16 and then 0.20 decreased 56-day compressive strength results from an initial 67.9 MPa to 57.4 MPa and then 34.2 MPa, respectively. Lower w/b ratios reduced water content and increased cement content, which contributed to completed compaction, adequate curing of paste samples, and, subsequently, better strength values. Furthermore, modification of the tailing paste with by-products was found to affect strength development in the paste specimens positively. As shown in Fig. 5c, increasing the GGBFS content remarkably influenced compressive strength in the paste samples, with large declines in early curing ages. In later ages, the paste samples with 10% GGBFS exhibited slightly increased strength compared with the control

mixture containing no GGBFS. This finding is likely due to the support by the GGBFS particles of the pozzolanic reaction at later curing ages. At higher levels of GGBFS replacement (30% and 50%), strength values declined, respectively, to 60.3 MPa and 37.4 MPa at 56 days of curing age, compared to 67.9 MPa in the control mixture without GGBFS. The reduction in OPC content and the lower reactivity of the GGBFS particles compared to OPC retarded the cement paste hydration process, leading to the presentation of large un-hydrated particles, which reduced compressive strength. Previous study, Hwang and Lin [41] illustrated that the both of level of GGBFS content and the age of curing time affect to the compressive strength of concrete samples. The compressive strength of GGBFS concrete (the replacement up to 40%) was comparable with normal concrete at 28-day of curing and continuously increased with curing time. Similar to other studies [42, 43], adding 5% SF was found in this study to significantly improve compressive strength at all test ages, increasing the amount of SF content beyond this level (i.e., to 10% and 15%) did not enhance strength development at early curing ages, even no strength within three days of curing. At later curing ages, incorporating SF addition had a beneficial influence to the compressive strength with an exceeding that of the control and the optimum amount of SF content at 5%. The contribution of SF to strength development may be explained by the high amorphous silica content of SF, which reacts with calcium hydroxide in OPC and GGBFS hydration products to form secondary C–S–H gel. Moreover, SF may be considered as a filler material that increases the packing of the solid phase in the cement paste structure and improves strength [44]. However, the incorporation with higher SF content (10 and 15%) reduced the compressive strength of paste samples compared with 5% SF level because of increasing water requirement and SP consumption. As shown in Table 2, incorporating 10% and 15% silica fume significantly increased SP amount, which may affect the hydration reaction and hardened matrix of paste specimens, resulting in lower compressive strength [42, 45].

## Thermal conductivity

To assess the hardened property of paste samples, thermal conductivity (TC) was measured at 7, 28, and 56 days of curing to evaluate the heat transfer by conduction through the paste specimens. In general, the microstructure and thermal characteristics of the components of a material significantly affects its TC results, with higher conductivity values indicating greater structural density and higher TC values for its constituents [46]. In this study, the TC result, showing increasing values over time, is presented in Table 3. The volume of hydration reaction gels increased with curing age, filling in the air voids, densifying the microstructure of the paste matrix, and increasing TC [47]. In terms of the effect of level of CT content, increasing the volume of CT to 40%, 50%, and 60% resulted in higher TC values of 1.30 W/m*k, 1.49 W/m*k, and 1.57 W/m*k, respectively, at 28 days of curing age. This result reflected an opposite trend with compressive strength, which showed reduced compressive strength with the addition of more CT ash content. Higher compressive strength was associated with greater TC in a previous study [48], inferring that the mine tailings alone are responsible for the increase in thermal conductivity of paste samples [34]. In addition, increasing the w/b ratio affected TC negatively. As shown in Table 3, the TC at 56 days of curing declined from 1.54 W/m*k to 1.41 W/m*k and 1.34 W/m*k with the w/b at 0.12, 0.16, and 0.20, respectively. The high water content is attributable to the presence of voids which retained water after hydration [49, 50], thus reducing the solid phase of paste specimens as well as reducing the TC value with an increasing water to binder ratio. Furthermore, the modification of the GGBFS resulted in thermal

**Table 3** Thermal conductivity results of tailing paste

| Mixtures | Thermal conductivity (W/m*k) | | | | | |
|---|---|---|---|---|---|---|
| | 7-day | Standard Deviation | 28-day | Standard Deviation | 56-day | Standard Deviation |
| 0.12T0.4S00F0 | 1.29 | 0.01 | 1.30 | 0.02 | 1.35 | 0.03 |
| 0.12T0.5S00F0 | 1.46 | 0.02 | 1.49 | 0.02 | 1.54 | 0.01 |
| 0.12T0.6S00F0 | 1.54 | 0.02 | 1.57 | 0.02 | 1.54 | 0.00 |
| 0.12T0.5S10F0 | 1.25 | 0.04 | 1.33 | 0.02 | 1.36 | 0.01 |
| 0.12T0.5S30F0 | 1.20 | 0.05 | 1.19 | 0.02 | 1.22 | 0.01 |
| 0.12T0.5S50F0 | 1.21 | 0.03 | 1.18 | 0.02 | 1.19 | 0.02 |
| 0.16T0.5S00F0 | 1.36 | 0.03 | 1.38 | 0.00 | 1.41 | 0.03 |
| 0.20T0.5S00F0 | 1.23 | 0.04 | 1.25 | 0.01 | 1.34 | 0.05 |
| 0.12T0.5S30F5 | 1.34 | 0.01 | 1.38 | 0.07 | 1.40 | 0.03 |
| 0.12T0.5S30F10 | 1.26 | 0.04 | 1.33 | 0.013 | 1.34 | 0.07 |
| 0.12T0.5S30F15 | 1.16 | 0.01 | 1.15 | 0.01 | 1.17 | 0.03 |

conductivity decreasing over the entire range of substitution across curing age. The GGBFS showed the latent hydration reaction and lower hydraulic activity index [51], which may be used to discuss the compressive strength and TC reduction in this study. Finally, using SF to modify the tailing paste significantly increased the TC testing results. As shown in Table 3, the TC results improved significantly with the addition of SF up to 10% and declined with the addition of 15% SF to a level that was below the control mixture without SF content. Thus, the mixture with 5% SF exhibited the highest TC. This result parallels the result for compressive strength, which significantly increased with SF level. The high hydraulic activity index of the amorphous silica in SF particles improves the pozzolanic reaction and structural density. Moreover, the fine particles of SF increased the packing of the solid phase by filling in the spaces between cement grains and improving the TC of paste specimens [44, 52].

## Ultrasonic pulse velocity (UPV)

UPV analysis was used in this study to assess the quality of paste samples by identifying the voids, cracks, and uniformity in internal structures. UPV test results have been used in many studies as an indicator of concrete and mortar specimen durability. Typically, UPV and compressive strength are associated, with higher UPV values corresponding with greater compressive strength [11, 53]. The UPV testing results for this study are shown in Fig. 6, with values increasing over curing time and rising relatively more quickly during the later curing ages, reaching a range of 3471–4520 m/s at 56 days of curing age. These results

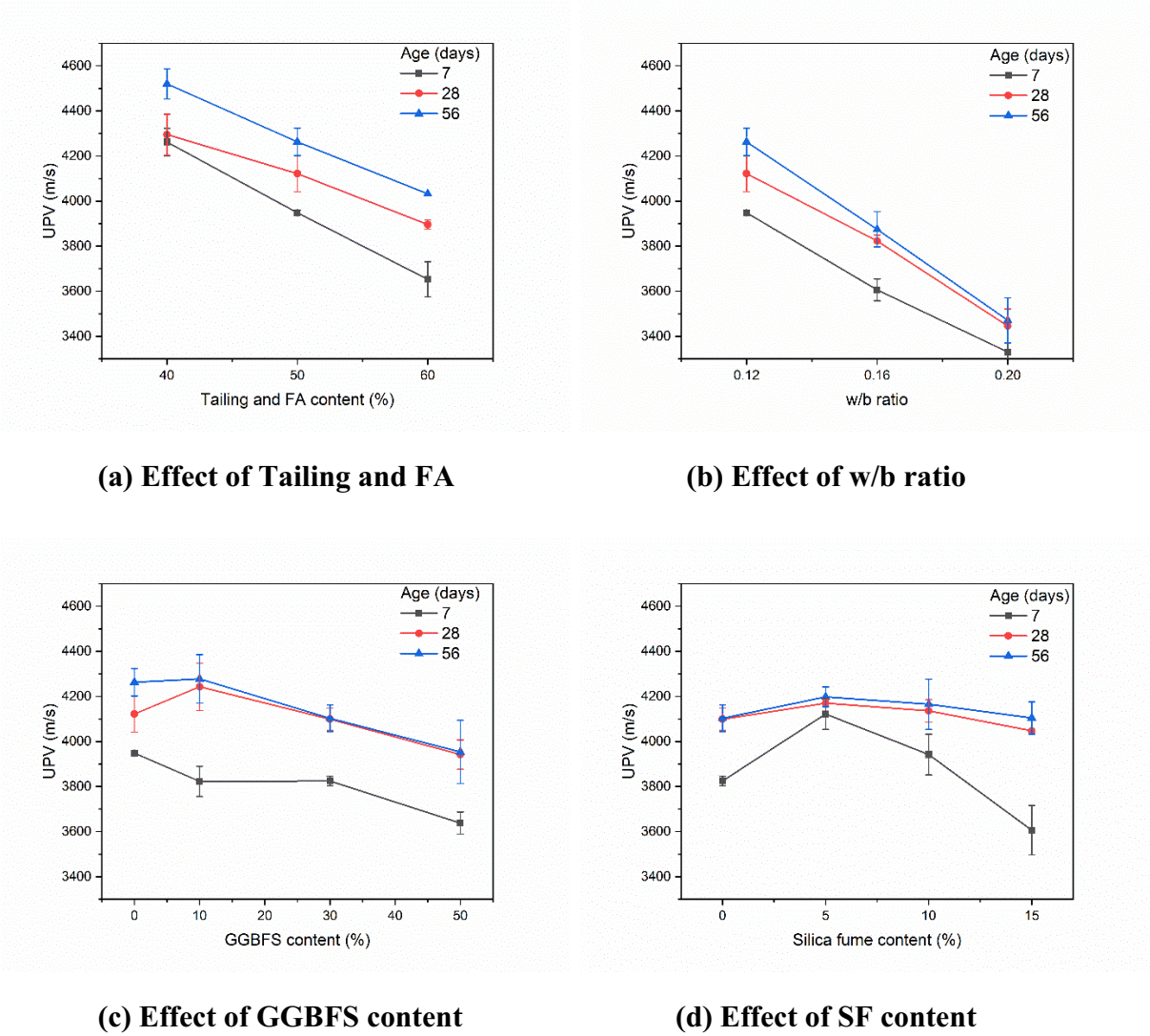


**Fig. 6** UPV results of tailing paste samples. **a** Effect of tailing and FA. **b** Effect of w/b ratio. **c** Effect of GGBFS content. **d** Effect of SF content

illustrate that UPV decreased significantly with increased CT volume and increased w/b ratio. Higher CT ratio and higher w/b ratio were shown to correspond with greater porosity and reduced the solid phase, which significantly affected the UPV results. Moreover, the lower cement content also affected the hydration process, which may also have contributed to the lower compressive strength and UPV values of the paste samples [54].

The modification of GGBFS and SF significantly affected the UPV of the paste specimens. At early ages, using GGBFS as a partial replacement for OPC negatively affected UPV, with reductions ranging from 3.1 to 7.9% at 10% to 50% GGBFS content. However, after 28 days of curing, the 10% GGBFS mixture exhibited the highest UPV result of all GGBFS levels. This performance correlates with the compressive strength result. In addition, the use of SF improved the UPV results of the paste specimens remarkably, with UPV values 0.02% to 2.3% higher at 56 days of curing age for specimens incorporating 15% to 5% SF, respectively. This performance is explained by the amorphous nature of SF leading to the progressive formation of additional C–S–H gels, which increases the solid phase and densifies the paste samples, thus improving compressive strength and UPV results [55].

## Water absorption

The water absorption (WA) test results for the paste mixtures at 28 and 56 days of curing age, illustrated in Fig. 7, show an expected decline with age. The water absorption

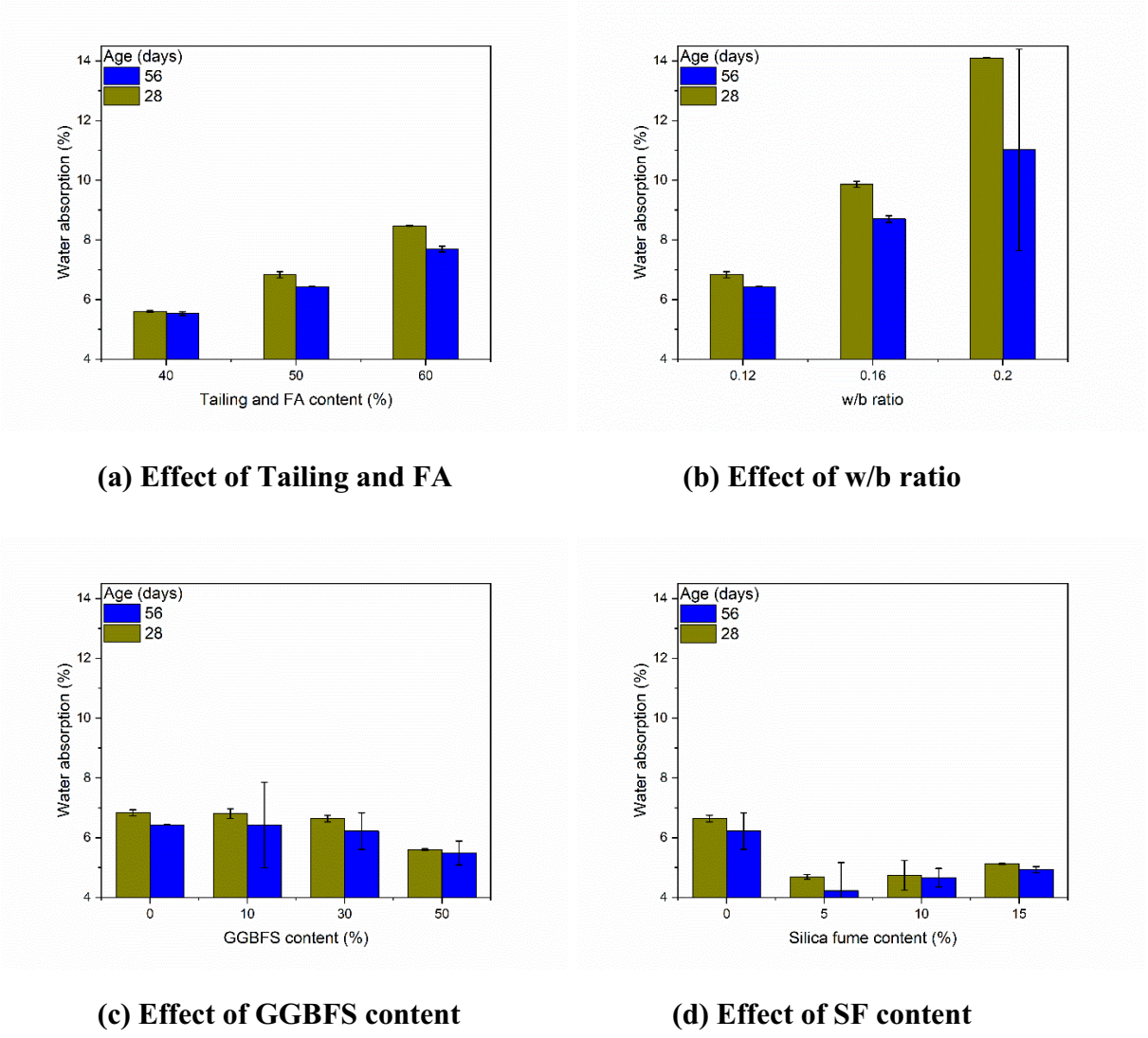


**Fig. 7** Water absorption of tailing paste samples. **a** Effect of tailing and FA. **b** Effect of w/b ratio. **c** Effect of GGBFS content. **d** Effect of SF content

of paste specimens is related to the internal pore structure and formation of cracks, which are, respectively, associated with the hydration process and the reactivity of the components. The development over time of the microstructure due to the hydration reaction increased compressive strength and reduced porosity and water absorption in the paste specimens [11]. As shown in Fig. 7a, higher volumes of the CT mixture increased water absorption. At volumes of 40%, 50%, and 60% of the paste samples, WA was 5.53%, 6.43%, and 7.69%, respectively, at 56 days of curing age. The low reactivity of FA and tailing particles may contribute significantly to the higher porosity structure and water absorption results in the specimens with higher CT volumes [56]. In addition, the reduction of cement content affected the hydration process and reduced the density of paste specimens, which may be another factor underlying the higher WA results in samples with higher volumes of CT [57]. Furthermore, increasing the w/b ratio was found to increase the water absorption results significantly. Mixtures with w/b ratios of 0.16 and 0.20 respectively exhibited WA values of 8.7% and 11.2% at 56 days of curing age, which were significantly higher than the WA value of mixture 0.12T0.5S00F0 (6.43%). The mixture without slag content (0.12T0.5S00F0) was further modified with different proportions of GGBFS and SF content to improve paste specimen properties. As expected, these specimens exhibited slightly reduced water absorption at higher levels of GGBFS content because the GGBFS particles, which are finer than those of OPC, filled in the micro pores in the cement paste that would otherwise be available to absorb water [58]. At 56 days of curing age, the water absorption of paste specimens was 6.43%, 6.42%, 6.22%, and 5.49% at 0%, 10%, 30%, and 50% GGBFS replacement, respectively. Moreover, using SF significantly improved the microstructure and reduced the water absorption of the paste mixtures. As detailed in Fig. 7d, the paste samples modified with different levels of SF exhibited 20.7–32% less water absorption than the paste without SF content, with the 5% SF sample returning the lowest WA value and 10% and 15% SF samples showing slightly higher WA values. The role of SF in water absorption is explained by its filling in of pore structures and its effect on the pozzolanic reaction. This finding for WA agrees with the above-mentioned findings for compressive strength performance.

## Sulfate attack resistance

Cementitious materials generally expand when they react with environmental sulfate due to their gypsum and ettringite, which promotes deterioration of the material and harms the long-term performance of paste samples [59]. Typically, the sulfate ions react with hydration products in cement, resulting in expansion, cracking, spalling, and concrete strength loss or mass change [6, 11]. In this study, the 28-day paste specimens were immersed in $Na_2SO_4$-5% concentration and the mass change performance of the paste specimens was measured using 10 wetting and drying cycles to evaluate sulfate resistance. As presented in Fig. 8, the mass of all of the tailing paste specimens had increased after 10 cycles. The raw materials contributed to the pozzolanic reactivity between the cementitious materials with sodium sulfate solution to create more hydration gels, which resulted in a denser microstructure and increased mass [11, 60, 61]. The effect of CT volume was insignificant, although higher volumes resulted in mass gain, as shown in Fig. 8a. In addition, the high w/b ratio specimens exhibited a sharp drop in mass after the first round and then steadily increased through subsequent rounds, while, the mass of the 0.12T0.5S00F0 mixture (w/b at 0.12) increased continuously. This difference may be explained by the steady evaporation of the high water volume retained in the higher w/b ratio samples after the first burning cycle, which decreased the mass of the tailing paste specimens. Moreover, the specimens with higher levels of GGBFS content exhibited more significant gains in mass due to the slow reaction of GGBFS and remained the high amount of un-hydrated particles, which reacted with sulfate environment to increase the mass. In addition, the effect of SF on mass change of paste samples is shown in Fig. 8d. The mass increased at the first cycle and became stable with testing time. The good pozzolanic reaction of SF particles resulted in their dense and discontinuous pore structure [42, 62], which prevented the movement of sulfate ions attack and reduced the formation of ettringite and gypsum in the paste matrix, resulting in a stable weight of paste specimens.

## SEM images' observation

In this study, the microstructure of the paste specimens was observed using secondary electron microscope (SEM) imaging of the paste specimens at 28 days of curing age. These SEM images, shown in Figs. 9 and 10, highlight the differences in morphological and microstructural features of the hardened paste samples modified by various admixtures. As shown in Fig. 9, the fine fly ash particles of different sizes, which were scattered throughout the paste matrix, blended with the hydration gels of C–S–H or C–A–S–H to support the further compaction of microstructure of the paste samples. Increasing the volume of tailing and fly ash reduced the density of the microstructure, resulting in higher numbers of entrapped air voids and un-hydrated particles due to their low pozzolanic reactivity [25]. In addition, increasing the w/b ratio increased water retention, with water gathering around un-hydrated particles, increasing matrix porosity (Fig. 10a and b). Adding GGBFS to reduce the use of cement was not found to reduce compression strength significantly. Thus, the paste samples exhibited essentially the similar features using 30% GGBFS to replace OPC, as displayed in

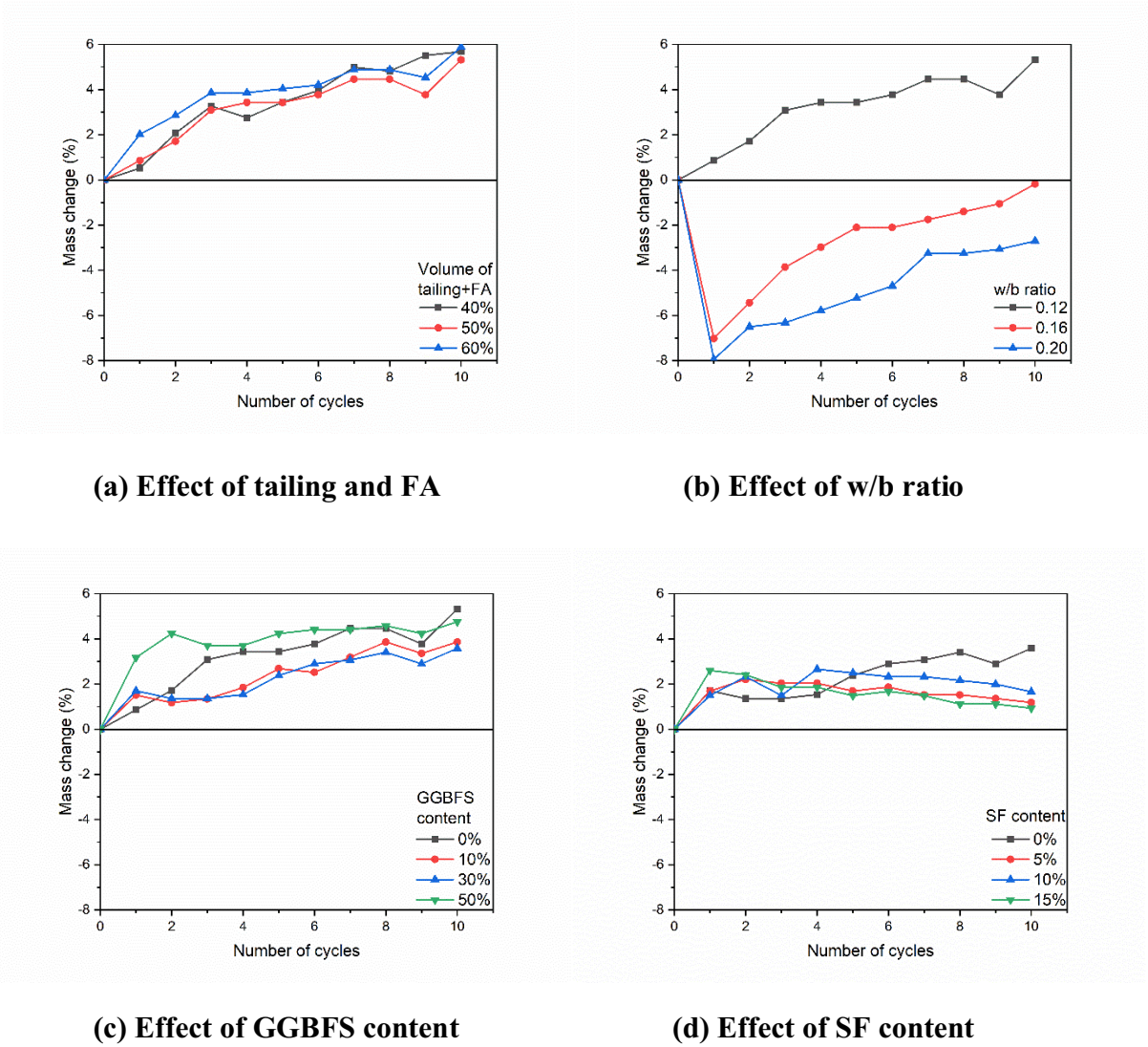


**Fig. 8** Mass change of tailing paste specimens exposed to 5% $Na_2SO_4$ solution. **a** Effect of tailing and FA. **b** Effect of w/b ratio. **c** Effect of GGBFS content. **d** Effect of SF content

Fig. 10a and c. Finally, adding SF remarkably improved the morphology of the paste specimens. Furthermore, in line with the compressive strength results, the filling effect and high pozzolanic reactivity of the SF particles remarkably increased the structural compactness of the specimens, as shown in Fig. 10d [25, 63].

## Conclusions

The following conclusions may be drawn from the results of this investigation:

1) The compressive strength of tailing paste increased over curing time to 34.2–86.2 MPa at 56 days of curing age. Lower compressive strength was associated with the incorporation of higher volumes of tailing and fly ash, higher GGBFS ratios, and higher w/b ratios. The tailing paste specimens that were modified using 5% silica fume exhibited significantly improved compressive strength.
2) The thermal conductivity of tailing paste increased with increasing tailing and FA volume, while thermal conductivity decreased with increasing GGBFS content and w/b ratio. In addition, the 5% SF specimen improved thermal conductivity of paste sample. However, high SF content level negatively affected the TC value of the specimens with added tailing paste.
3) The UPV and water absorption results for the tailing paste samples exhibited an inverse trend, with the UPV values improving (to 3471–4520 m/s at 56 days of cur-

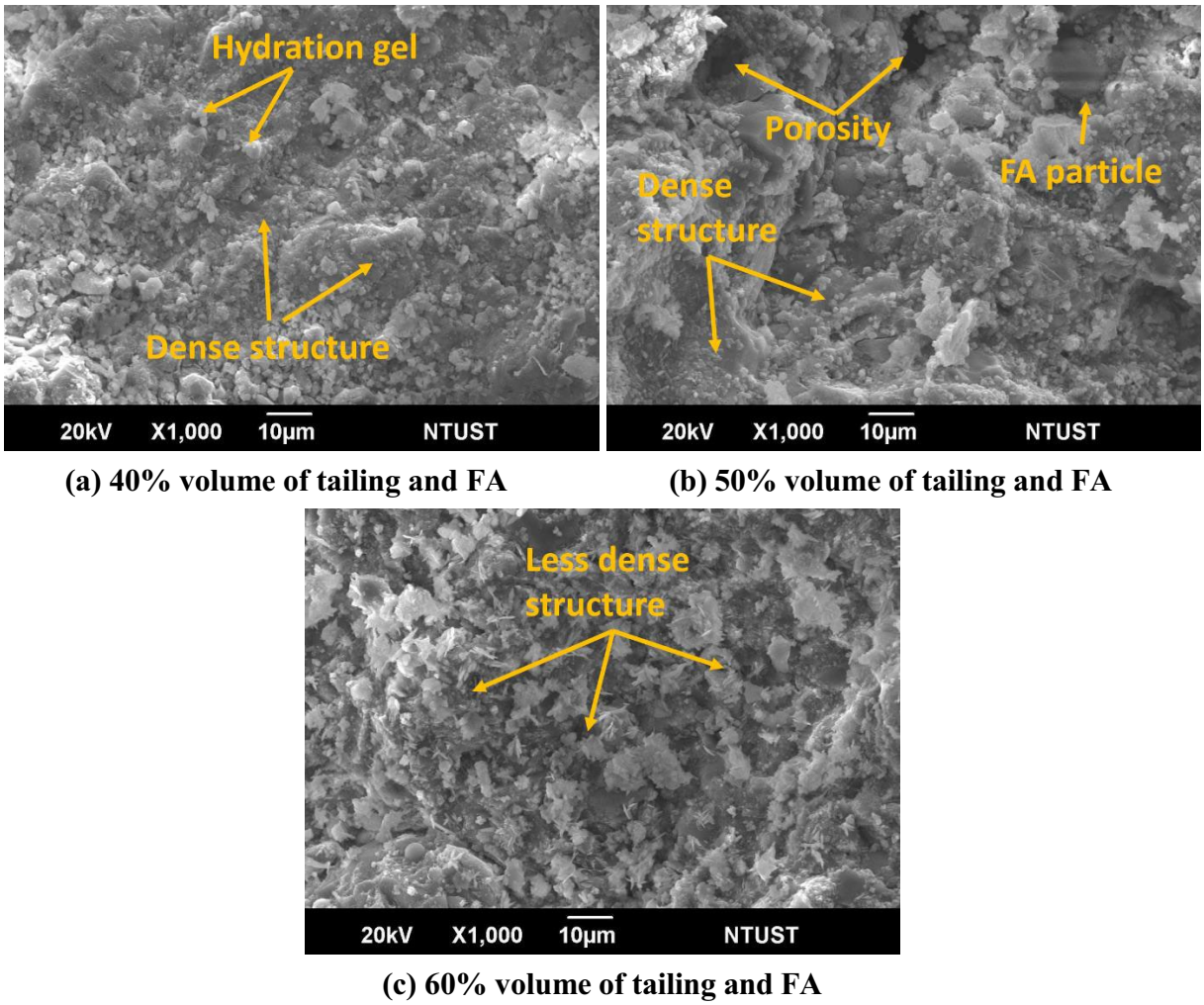


**Fig. 9** SEM images of tailing paste with different tailing content volumes. **a** 40% volume of tailing and FA, **b** 50% volume of tailing and FA, **c** 60% volume of tailing and FA

ing age) and water absorption decreasing with curing age. Increasing the tailing and FA content, GGBFS level, and w/b ratio did not improve to the UPV result and increased water absorption. The 5% SF specimen achieved a better UPV result with a reduction in water absorption.

4) Tailing paste performed well under sulfate attack. After the series of 10 wetting–drying immersion cycles in sodium sulfate solution, the mass of the tailing paste increased due to the pozzolanic reaction between the cementitious materials and the sodium sulfate solution.
5) The SEM analysis found that the tailing paste exhibited a homogeneous and compacted microstructure at 28 days of curing age. Lower structural density was found at higher levels of tailing and fly ash volume and at higher w/b ratios. Partially replacing 30% of OPC with GGBFS did not affect the microstructure significantly. Finally, adding 5% SF improved the microstructure and the hardened properties of tailing paste samples significantly.

The use of high-volume mine tailing in the manufacturing of composite binder has a usually detrimental impact on the characteristics of the paste specimens. However, the tailing paste samples with modified by-products exhibited good hardened properties and sulfate attack resistance. This study demonstrated proficiency in using a high volume of mine tailing with by-products in a composite binder, performing good properties, and eventually giving a solution for sustainable development.

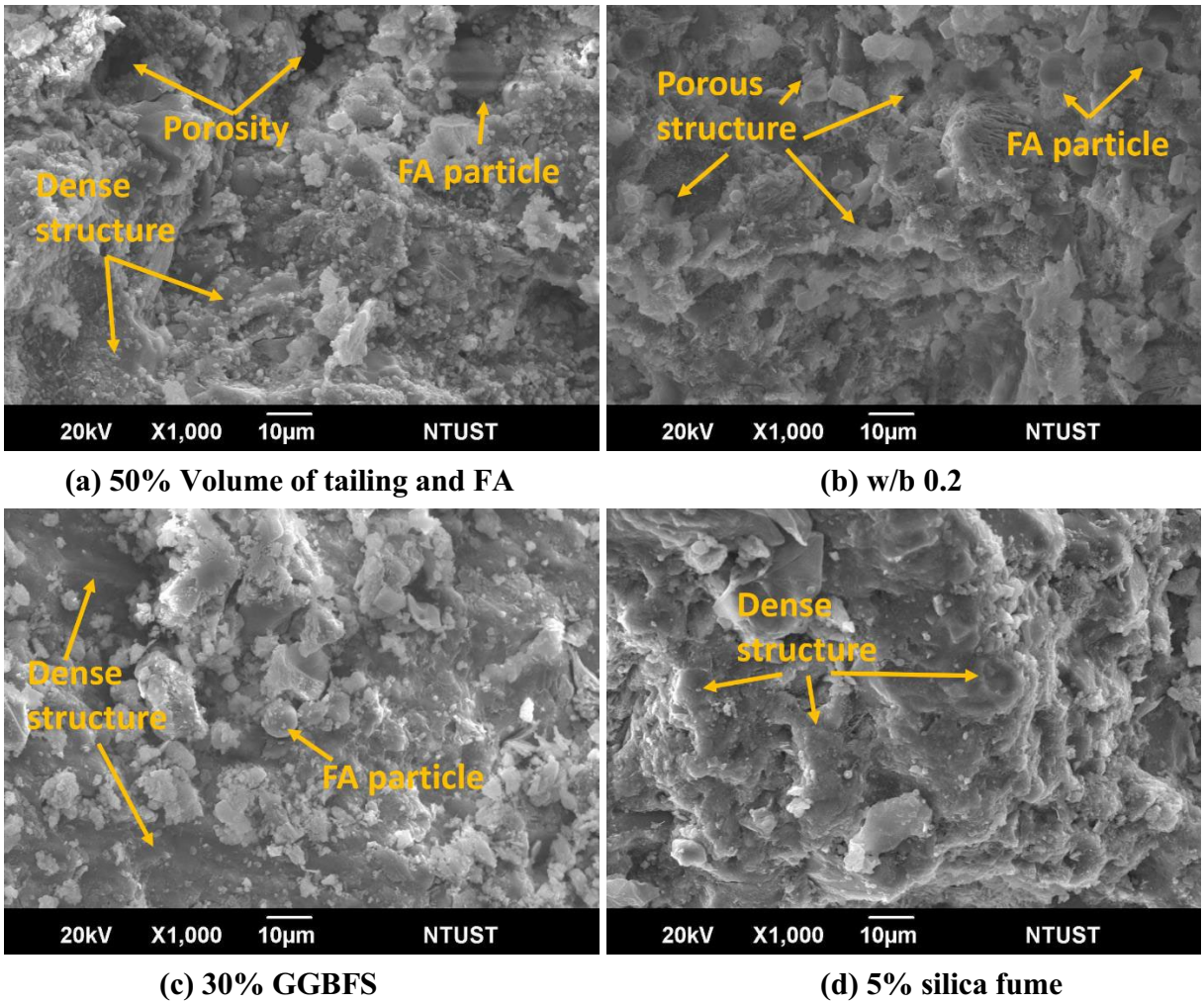


**Fig. 10** SEM images of tailing modified with various by-products. **a** 50% volume of tailing and FA, **b** w/b-0.2, **c** 30% GGBFS, **d** 5% silica fume

**Acknowledgements** This research was conducted at the Construction Material Research Laboratory (CMRL) of the National Taiwan University of Science and Technology (NTUST) with valuable support from the Taiwan Building Technology Center, MOST and MOE.

## References

1. Damtoft JS, Lukasik J, Herfort D, Sorrentino D, Gartner EM (2008) Sustainable development and climate change initiatives. Cem Concr Res 38(2):115–127
2. Scrivener KL, Kirkpatrick RJ (2008) Innovation in use and research on cementitious material. Cem Concr Res 38(2):128–136
3. Benhelal E, Zahedi G, Shamsaei E, Bahadori A (2013) Global strategies and potentials to curb CO2 emissions in cement industry. J Clean Prod 51:142–161
4. Li J, Tharakan P, Macdonald D, Liang X (2013) Technological, economic and financial prospects of carbon dioxide capture in the cement industry. Energy Policy 61:77–87
5. Leemann A, Loser R (2011) Analysis of concrete in a vertical ventilation shaft exposed to sulfate-containing groundwater for 45years. Cement Concr Compos 33(1):74–83
6. González MA, Irassar EF (1997) Ettringite formation in low C3A portland cement exposed to sodium sulfate solution. Cem Concr Res 27(7):1061–1071
7. Idiart AE, López CM, Carol I (2011) Chemo-mechanical analysis of concrete cracking and degradation due to external sulfate attack: A meso-scale model. Cement Concr Compos 33(3):411–423
8. Neville A (2004) The confused world of sulfate attack on concrete. Cem Concr Res 34(8):1275–1296
9. Duran Atiş C, Bilim C (2007) Wet and dry cured compressive strength of concrete containing ground granulated blast-furnace slag. Build Environ 42:3060–3065
10. Durán-Herrera A, Juárez CA, Valdez P, Bentz DP (2011) Evaluation of sustainable high-volume fly ash concretes. Cement Concr Compos 33:39–45
11. Huynh TP, Vo DH, Hwang CL (2018) Engineering and durability properties of eco-friendly mortar using cement-free SRF binder. Constr Build Mater 160:145–155
12. Hwang CL, Bui LAT, Chen CT (2011) Effect of rice husk ash on the strength and durability characteristics of concrete. Constr Build Mater 25:3768–3772

13. Elahi MMA, Shearer CR, Reza ANR, Saha AK, Khan MNN, Hossain MM, Sarker PK (2021) Improving the sulfate attack resistance of concrete by using supplementary cementitious materials (SCMs): A review. Constr Build Mater 281:122628
14. Wainwright PJ, Rey N (2000) The influence of ground granulated blastfurnace slag (GGBS) additions and time delay on the bleeding of concrete. Cement Concr Compos 22:253–257
15. Demirboğa R, Türkmen İ, Karakoç MB (2004) Relationship between ultrasonic velocity and compressive strength for high-volume mineral-admixtured concrete. Cem Concr Res 34:2329–2336
16. El-Chabib H, Syed A (2013) Properties of self-consolidating concrete made with high volumes of supplementary cementitious materials. J Mater Civ Eng 25:1579–1586
17. Jeong Y, Park H, Jun Y, Jeong J-H, Oh JE (2015) Microstructural verification of the strength performance of ternary blended cement systems with high volumes of fly ash and GGBFS. Constr Build Mater 95:96–107
18. Kuder K, Lehman D, Berman J, Hannesson G, Shogren R (2012) Mechanical properties of self consolidating concrete blended with high volumes of fly ash and slag. Constr Build Mater 34:285–295
19. Gou M, Zhou L, Then N (2019) Utilization of tailings in cement and concrete: a review. Sci Eng Compos Mater 26:449–464
20. Feng Q, Wen S, Deng J, Zhao W (2017) Combined DFT and XPS investigation of enhanced adsorption of sulfide species onto cerussite by surface modification with chloride. Appl Surf Sci 425:8–15
21. Feng Q, Zhao W, Wen S, Cao Q (2017) Activation mechanism of lead ions in cassiterite flotation with salicylhydroxamic acid as collector. Sep Purif Technol 178:193–199
22. Feng Q, Zhao W, Wen S (2018) Surface modification of malachite with ethanediamine and its effect on sulfidization flotation. Appl Surf Sci 436:823–831
23. Zhao Y, Zhang Y, Liu T, Chen T, Bian Y, Bao S (2013) Preconcentration of vanadium from stone coal by gravity separation. Int J Miner Process 121:1–5
24. Zhang X, Tan X, Yi Y, Liu W, Li C (2017) Recovery of manganese ore tailings by high-gradient magnetic separation and hydrometallurgical method. JOM. https://doi.org/10.1007/s11837-017-2521-5
25. Zhao S, Fan J, Sun W (2014) Utilization of iron ore tailings as fine aggregate in ultra-high performance concrete. Constr Build Mater 50:540–548
26. Sun W, Wang H, Hou K (2018) Control of waste rock-tailings paste backfill for active mining subsidence areas. J Clean Prod 171:567–579
27. Panchal S, Deb D, Sreenivas T (2018) Mill tailings based composites as paste backfill in mines of U-bearing dolomitic limestone ore. J Rock Mechan Geotech Eng 10:310–322
28. Jiao RM, Xing P, Wang CY, Ma BZ, Chen YQ (2017) Recovery of iron from copper tailings via low-temperature direct reduction and magnetic separation: process optimization and mineralogical study. Int J Miner Metall Mater 24:974–982
29. Lü C, Wang Y, Qian P, Liu Y, Fu G, Ding J, Ye S, Chen Y (2018) Separation of chalcopyrite and pyrite from a copper tailing by ammonium humate. Chin J Chem Eng 26:1814–1821
30. Xi X, Zhang C, Zhou T, Zhu H, Li Y, Xu Z (2014) Effect of copper tailings on burn-ability of cement raw meal and performances of clinker. Jianzhu Cailiao Xuebao J Build Mater 17:1102–1107
31. Jian S, Gao W, Lv Y, Tan H, Li X, Li B, Huang W (2020) Potential utilization of copper tailings in the preparation of low heat cement clinker. Constr Build Mater 252:119–130
32. Liu S, Wang L, Li Q, Song J (2020) Hydration properties of Portland cement-copper tailing powder composite binder. Constr Build Mater 251:118882
33. Onuaguluchi O, Eren Ö (2012) Recycling of copper tailings as an additive in cement mortars. Constr Build Mater 37:723–727
34. Onuaguluchi O, Eren Ö (2012) Durability-related properties of mortar and concrete containing copper tailings as a cement replacement material. Mag Concr Res 64:1015–1023
35. Dandautiya R, Singh AP (2019) Utilization potential of fly ash and copper tailings in concrete as partial replacement of cement along with life cycle assessment. Waste Manage 99:90–101
36. Zheng K, Zhou J, Gbozee M (2015) Influences of phosphate tailings on hydration and properties of Portland cement. Constr Build Mater 98:593–601
37. Kundu S, Aggarwal A, Mazumdar S, Dutt B (2016) Stabilization characteristics of copper mine tailings through its utilization as a partial substitute for cement in concrete: preliminary investigations. Environm Earth Sci 75:1–9
38. Cheng Y, Huang F, Li W, Liu R, Li G, Wei J (2016) Test research on the effects of mechanochemically activated iron tailings on the compressive strength of concrete. Constr Build Mater 118:164–170
39. Han F, Li L, Song S, Liu J (2017) Early-age hydration characteristics of composite binder containing iron tailing powder. Powder Technol 315:322–331
40. Wong RCK, Gillott JE, Law S, Thomas MJ, Poon CS (2004) Calcined oil sands fine tailings as a supplementary cementing material for concrete. Cem Concr Res 34:1235–1242
41. Hwang CL, Lin CY (1986) Strength development of blended blast-furnace slag-cement mortars. J Chin Inst Eng 9:233–239
42. Bingöl AF, Haghghipour Balaneji H (2018) Determination of sulfate resistance of concretes containing silica fume and fly ash. Iran J Sci Technol Transact Civil Eng. https://doi.org/10.1007/S40996-018-0160-X
43. Abo-El-Enein SA, El-kady G, El-sokkary TM, Gharieb M (2014) Physico-mechanical properties of composite cement pastes containing silica fume and fly ash. HBRC J. https://doi.org/10.1016/j.hbrcj.2014.02.003
44. Elahi A, Basheer PAM, Nanukuttan SV, Khan QUZ (2010) Mechanical and durability properties of high performance concretes containing supplementary cementitious materials. Constr Build Mater 24:292–299
45. Sezer G (2012) Compressive strength and sulfate resistance of limestone and/or silica fume mortars. Constr Build Mater 26:613–618
46. Asadi I, Shafigh P, Abu Hassan ZFB, Mahyuddin NB (2018) Thermal conductivity of concrete – A review. J Build Eng 20:81–93
47. Uysal M, Yilmaz K (2011) Effect of mineral admixtures on properties of self-compacting concrete. Cement Concr Compos 33:771–776
48. Hwang CL, Tran VA (2016) Engineering and durability properties of self-consolidating concrete incorporating foamed lightweight aggregate. J Mater Civ Eng 28:04016075
49. Brito J, Robles R (2010) Recycled aggregate concrete (RAC) methodology for estimating its long-term properties. Indian J Eng Mater Sci 17:449–462
50. Evangelista L, Brito J (2018) Concrete with fine recycled aggregates: A review. Eur J Environm Civil Eng 18(2):129–172
51. Hadj-sadok A, Kenai S, Courard L, Darimont A (2011) Microstructure and durability of mortars modified with medium active blast furnace slag. Constr Build Mater 25:1018–1025
52. Aldred J, Holland TC, Morgan DR (2006) Guide for the use of silica fume in concrete. Architect 234
53. Bogas JA, Gomes MG, Gomes A (2013) Compressive strength evaluation of structural lightweight concrete by non-destructive ultrasonic pulse velocity method. Ultrasonics 53:962–972
54. Thomas BS, Damare A, Gupta RC (2013) Strength and durability characteristics of copper tailing concrete. Constr Build Mater 48:894–900

55. Hwang CL, Damtie Yehualaw M, Vo DH, Huynh TP (2019) Development of high-strength alkali-activated pastes containing high volumes of waste brick and ceramic powders. Constr Build Mater 218:519–529
56. Esmaeili J, Aslani H (2019) Use of copper mine tailing in concrete: strength characteristics and durability performance. J Mater Cycles Waste Manage 21:729–741
57. Thomas J, Thaickavil NN, Wilson PM (2018) Strength and durability of concrete containing recycled concrete aggregates. J Build Eng 19:349–365
58. Sarathy R, Dhinakaran G (2014) Strength and durability characteristics of GGBFS based HPC. Asian J Appl Sci 7:224–231
59. Dung NT, Chang TP, Chen CT (2014) Engineering and sulfate resistance properties of slag-CFBC fly ash paste and mortar. Constr Build Mater 63:40–48
60. Lorenzo M, Goñi S, Bustos A (2001) Activation of pozzolanic reaction of hydrated portland cement fly ash pastes in sulfate solution. J Am Ceram Soc 85:3071–3075
61. Siad H, Kamali-Bernard S, Mesbah HA, Escadeillas G, Mouli M, Khelafi H (2013) Characterization of the degradation of self-compacting concretes in sodium sulfate environment: Influence of different mineral admixtures. Constr Build Mater 47:1188–1200
62. Torii K, Kawamura M (1994) Effects of fly ash and silica fume on the resistance of mortar to sulfuric acid and sulfate attack. Cem Concr Res 24:361–370
63. Scrivener KL, Bentur A, Pratt PL (1988) Quantitative characterization of the transition zone in high strength concretes. Adv Cem Res 1:230–237